

A PROBABILISTIC APPROACH TO CLOCK SYNCHRONIZATION OF CASCADED NETWORK ELEMENTS

Chongning Na, Dragan Obradovic, Ruxandra Lupas Scheiterer

Siemens AG, Corporate Technology, Information and Communications, Munich, Germany

ABSTRACT

Precision Time Protocol (PTP) synchronizes clocks of networked elements by exchanging messages containing precise time-stamps. Based on the available timing information, different algorithms can be developed for the clock synchronization. This paper introduces a novel PTP-based method in which clock synchronization is formulated as a probabilistic inference problem and is solved by Kalman filtering. The performance of this approach is verified by numerical results.

Index Terms— Clock synchronization, Precision Time Protocol, probabilistic model, Kalman filter

1. INTRODUCTION

Ethernet-based applications usually require the networked clocks to be synchronized. The Standard Network Time Protocol (NTP) [1], [2], executed over Ethernet provides synchronization accuracy at the millisecond level, which is appropriate for processes that are not time critical. However, in many applications, for example base station synchronization or motion control, where only sub-microsecond level synchronization errors are allowed, a more accurate synchronization solution is needed. The Precision Time Protocol (PTP), delivered by the IEEE 1588 standard [3] published in 2002 is a promising Ethernet synchronization protocol. It was enhanced by the transparent clock (TC) concept, introduced in [4], which has been adopted in the new version of IEEE 1588 published in 2007 (IEEE 1588 version 2 was approved by the IEEE on March 27, 2008). After running the “Best Master Algorithm”, which determines the so-called “*master*” clock, messages carrying precise timing information are periodically transmitted by the master and propagated by the so-called “*slave*” clocks after acquiring and updating the contained timing information. Intermediate bridges have to be “IEEE-1588-conform”, i.e. are network components with known delay.

Factors that affect the synchronization quality achievable by PTP include the stability of oscillators, the resolution and precision of time stamping the message, the frequency of sending synchronization messages, and the propagation

delay variation caused by the jitter in the intermediate elements. Some analytical work has been presented in [5][6] to show the influence of these factors on the synchronization accuracy. It can be seen from the analytical results that stamping imprecision, including quantization error and stamping jitters, have very adverse effects because the errors introduced by different elements accumulate along the network. On the other hand, each clock in the network is a dynamic system. Clock synchronization can be formulated as a state estimation of dynamic systems. This paper uses a state-space model to describe the synchronization problem and solve it using a Kalman filter. The whole paper is organized as follows. Section 2 introduces the IEEE 1588 peer-to-peer system model analyzed in this paper and briefly describes the PTP protocol. Section 3 derives the state-space model for the networked clock synchronization. Simulation results are shown in section 4 to verify the performance of the state-space model and the Kalman filter. Finally, Section 5 concludes the paper.

2. PRECISION TIME PROTOCOL

Fig. 1 shows a system with $N+1$ cascaded elements connected in a line topology. The PTP has a master/slave structure. $N+1$ elements are connected one by one to form a network with a line topology. The first element is the time source, also called (grand)master, which provides the reference time to the rest N elements, called slave elements.

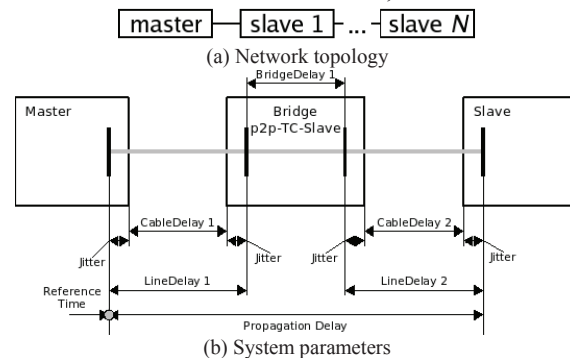


Fig. 1. System model

Fig. 2 illustrates the messages defined in PTP for the time synchronization. The master element periodically sends Sync messages which carry the (time)counter state of the

master clock M^i , stamped at the sending time, and are propagated along the network. Quantities, certain or not, linked with the Sync message transmitted by the master at time t_i are labeled by the superscript i . Upon the reception of a Sync message, a slave, e.g. slave n , records according to its own clock the reception time S_n^i . Each time a time-stamp is read, a jitter ξ of known distribution is incurred, e.g. due to the quantizing effect of having to wait for the next rising edge of the logic circuitry. A time labeled by S_n (resp. M) means “measured in the local time of slave n (resp. master time)”; a tilde on a symbol means measurement corrupted by jitter, e.g. $\tilde{S}_n^i = S_n^i + \xi_n^i$; a hat on a symbol means “estimate”.

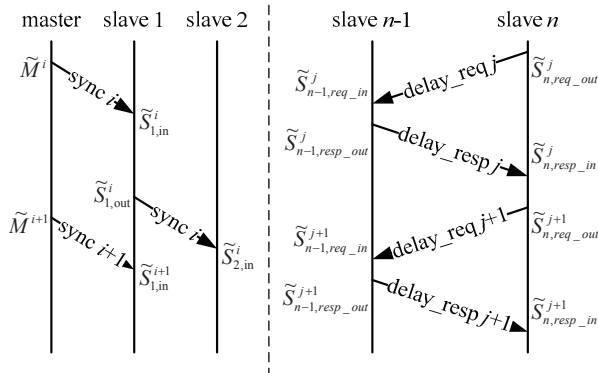


Fig. 2. PTP Messages

The *line delay* LD_n^i , is the propagation time between the n^{th} slave and its uplink element, and is estimated by using the “line delay estimation process”. The Sync message is forwarded after a *bridge delay* BD_n^i , which is recorded at each slave as the difference of the times stamped at reception and forwarding. Slave n forwards the Sync message to the next slave. An estimate of the master counter state at the time of forwarding is transmitted to slave $n+1$ for its own estimation of master time.

Time intervals measured by two different clocks will be called “skewed”. To be able to add or subtract them from each other they have to be converted to the same time basis. To this end each slave determines its frequency offset to the master. The *rate compensation factor* (RCF, also “rate ratio”) is defined as the frequency ratio of two clocks. We use $RCF_{X/Y}$ to denote the estimated frequency ratio between X and Y , i.e. ideally $RCF_{X/Y} = f_X/f_Y$.

The estimation of the line delay to the predecessor is shown on the right in Fig. 2; j indexes the line delay computation. This process uses 4 time-stamps: with periodicity R , node n (the requestor) sends a request message to node $n-1$ and records its time of departure, \tilde{S}_{n,req_out}^j (1st). Node $n-1$ (the responder) reports the two time-stamps of

receiving the request message and transmitting the reply: \tilde{S}_{n-1,req_in}^j and $\tilde{S}_{n-1,resp_out}^j$ (2nd and 3rd). The *responder delay* of node $n-1$ is RD_{n-1}^j in absolute time, and is in local time:

$$\hat{S}_{n-1,respD}^j := \tilde{S}_{n-1,resp_out}^j - \tilde{S}_{n-1,req_in}^j \quad (1)$$

Node n records the time, $\tilde{S}_{n,resp_in}^j$ (4th), of receiving the desired reply, after a *requestor delay* in node n time of:

$$\hat{S}_{n,reqD}^j := \tilde{S}_{n,resp_in}^j - \tilde{S}_{n,req_out}^j \quad (2)$$

To be able to subtract the skewed time intervals of (1) and (2), each element maintains an “RCF peer” estimate, i.e. frequency ratio estimate to its predecessor, estimated via:

$$RCF_{S_n/S_{n-1}}^j = \frac{\tilde{S}_{n,req_out}^j - \tilde{S}_{n,req_out}^{j-1}}{\tilde{S}_{n-1,req_in}^j - \tilde{S}_{n-1,req_in}^{j-1}}, \quad (3)$$

Then the line delay can be estimated as:

$$\hat{S}_n(LD_n^j) = \frac{\tilde{S}_{n,reqD}^j - \tilde{S}_{n-1,respD}^j \cdot RCF_{S_n/S_{n-1}}^j}{2} \quad (4)$$

Usually several successive line delay estimates are averaged. The result of the averaged line delay estimates is the constant cable delay plus the mean of several i.i.d. random variables ξ_n^j . According to the *Central Limit Theorem*, for several summands this is well approximated by the cable delay plus additive Gaussian noise:

$$\hat{S}_n(LD_n^j) = S_n(CD) + v_n^j \quad (5)$$

3. STATE SPACE MODEL FOR CLOCK SYNCHRONIZATION

Clock synchronization at each slave builds a relationship between the slave clock and the master clock so that for any given slave counter value, the estimated master counter value at that time point can be calculated. To build such a relationship, we define a hidden state variable x_n^i that is the true master counter state corresponding to the slave time-stamp \tilde{S}_n^i . In the following sections, we will introduce a state space model from master to slave 1, and from slave n to slave $n+1$.

3.1. The Definition of Hidden States Variables

Figure 3 illustrates the relationship between counter state variables, observed or hidden.

$x_{n,in}^i$ resp. $x_{n,out}^i$ are defined as the (true) master counter values that correspond to the slave time-stamps $\tilde{S}_{n,in}^i$ resp. $\tilde{S}_{n,out}^i$, i.e., the time-stamps generated at the reception and forwarding of the i^{th} sync message. $M_{n,in}^i$ resp. $M_{n,out}^i$ are as the (true) master counter values that correspond to the true slave times $S_{n,in}^i$ resp. $S_{n,out}^i$.

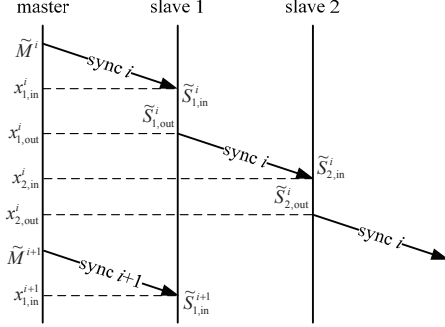


Fig. 3. Observed and hidden variables

3.2. State-Space Model: Master to Slave 1

It can be easily observed that $x_{n,in}^i - x_{n,in}^{i-1}$ and $\tilde{S}_{n,in}^i - \tilde{S}_{n,in}^{i-1}$ are the same time interval measured by different clocks, i.e., master clock and slave clock. They are related by the rate ratio of the two clocks, that is:

$$x_{n,in}^i - x_{n,in}^{i-1} = (\tilde{S}_{n,in}^i - \tilde{S}_{n,in}^{i-1}) \cdot \bar{R}_{M/S_n}^{[x_{n,in}^i, \tilde{S}_{n,in}^i]} \quad (6)$$

where $\bar{R}_{X/Y}^{[a,b]}$ denotes the averaged frequency ratio between element X and Y during the interval $[a, b]$.

The frequency ratio between master clock and slave 1 can be estimated by:

$$\begin{aligned} RCF_{M/S_1}^i &= \frac{\tilde{M}^i - \tilde{M}^{i-1}}{\tilde{S}_{1,in}^i - \tilde{S}_{1,in}^{i-1}} = \frac{M^i - M^{i-1} + \xi_M^i - \xi_M^{i-1}}{\tilde{S}_{1,in}^i - \tilde{S}_{1,in}^{i-1}} \\ &= \frac{(S_{1,in}^i - S_{1,in}^{i-1}) \cdot \bar{R}_{M/S_1}^{[S_{1,in}^i, S_{1,in}^{i-1}]} + \xi_M^i - \xi_M^{i-1}}{\tilde{S}_{1,in}^i - \tilde{S}_{1,in}^{i-1}} \\ &\approx \frac{(S_{1,in}^i - S_{1,in}^{i-1}) \cdot \bar{R}_{M/S_1}^{[S_{1,in}^i, S_{1,in}^{i-1}]} + \xi_M^i - \xi_M^{i-1}}{\tilde{S}_{1,in}^i - \tilde{S}_{1,in}^{i-1}} \quad (7) \\ &= \frac{(\tilde{S}_{1,in}^i - \tilde{S}_{1,in}^{i-1} - \xi_{S_{1,in}}^i + \xi_{S_{1,in}}^{i-1}) \cdot \bar{R}_{M/S_1}^{[S_{1,in}^i, S_{1,in}^{i-1}]} + \xi_M^i - \xi_M^{i-1}}{\tilde{S}_{1,in}^i - \tilde{S}_{1,in}^{i-1}} \\ &\approx \frac{(\tilde{S}_{1,in}^i - \tilde{S}_{1,in}^{i-1}) \cdot \bar{R}_{M/S_1}^{[S_{1,in}^i, S_{1,in}^{i-1}]} + \xi_M^i - \xi_M^{i-1} - \xi_{S_{1,in}}^i + \xi_{S_{1,in}}^{i-1}}{\tilde{S}_{1,in}^i - \tilde{S}_{1,in}^{i-1}} \\ &= \bar{R}_{M/S_1}^{[S_{1,in}^i, S_{1,in}^{i-1}]} + \frac{\xi_M^i - \xi_M^{i-1} - \xi_{S_{1,in}}^i + \xi_{S_{1,in}}^{i-1}}{\tilde{S}_{1,in}^i - \tilde{S}_{1,in}^{i-1}} \end{aligned}$$

The approximation made in the 3rd and 5th line in (7) is based on the fact that the stamping error is small and the frequency ratio is very close to 1 (maximum deviation from the nominal frequency is smaller than 100ppm). Since it is the sum of 4 i.i.d. RVs, we use the Gaussian RV $\eta^j \sim N(0, \mathcal{Q})$ to approximate the last term in (7). So (7) can be rewritten as:

$$RCF_{M/S_1}^i = \bar{R}_{M/S_1}^{[S_{1,in}^i, S_{1,in}^{i-1}]} + \frac{\eta^i}{\tilde{S}_{1,in}^i - \tilde{S}_{1,in}^{i-1}} \quad (8)$$

Inserting (8) into (6) and reformulating, we obtain:

$$x_{1,in}^i = x_{1,in}^{i-1} + (\tilde{S}_{1,in}^i - \tilde{S}_{1,in}^{i-1}) \cdot RCF_{M/S_1}^i - \eta_1^i \quad (9)$$

This constitutes *the state transition model*.

On the other hand, $x_{n,in}^i$ and M^i are related by the line delay:

$$\begin{aligned} M^i &= \tilde{M}^i - \xi_M^i = x_{1,in}^i - \xi_{S_{1,in}}^i - S_1(CD_1) \cdot R_{M/S_1}, \text{ so} \\ \tilde{M}^i &\approx x_{1,in}^i - \xi_{S_{1,in}}^i + \xi_M^i - [\hat{S}_1(CD_1^i) - \nu_1^i] \cdot (RCF_{M/S_1}^i) \quad (10) \\ &= x_{1,in}^i + \hat{S}_1(CD_1^i) \cdot RCF_{M/S_1}^i - \xi_{S_{1,in}}^i + \xi_M^i + RCF_{M/S_1}^i \cdot \nu_1^i \end{aligned}$$

The approximation made in the second line is based on the fact that the cable delay is usually very small so that it attenuates the error made in the RCF estimation. We can combine the last three terms in (10) and approximate it with a Gaussian RV $\varepsilon^j \sim N(0, U)$. So (10) can be written as:

$$\tilde{M}^i = x_{1,in}^i + \hat{S}_1(CD_1^i) \cdot RCF_{M/S_1}^i + \varepsilon_1^i \quad (11)$$

This constitutes *the observation model*.

The state-space model is presented by (9) and (11) and the estimation of hidden variable $x_{n,in}^i$ can be obtained by using a Kalman filter.

In order to enable slave 2 to estimate its hidden variables, slave 1 also estimates $x_{1,out}^i$ and transmits it to slave 2. The estimation of $x_{1,out}^i$ is given by, using (8) for the 2nd line:

$$\begin{aligned} x_{1,out}^i &= x_{1,in}^i + (\tilde{S}_{1,out}^i - \tilde{S}_{1,in}^i) \cdot \bar{R}_{M/S_1}^{[x_{1,out}^i, \tilde{S}_{1,out}^i]} \\ &= x_{1,in}^i + (\tilde{S}_{1,out}^i - \tilde{S}_{1,in}^i) \cdot \left(RCF_{M/S_1}^i - \frac{\eta_1^i}{\tilde{S}_{1,in}^i - \tilde{S}_{1,in}^{i-1}} \right) \quad (12) \end{aligned}$$

3.2. State-Space Model: Slave n to Slave $n+1$

Each slave element acts as a transparent element. It estimates the master counter state using (12) and passed this information to the next element so that the next element believes that it has received the time-stamps from the master clock itself. The slave transmits its estimate $\hat{x}_{n,out}^i$ as well as the variance thereof, $P_{n,out}^i$. The true master value is actually

$$X_{n,out}^i = \hat{x}_{n,out}^i + \gamma_{n,out}^i, \quad \text{for unknown } \gamma_{n,out}^i \sim N(0, P_{n,out}^i), \quad \text{and}$$

$$X_{n,out}^i - M_{n,out}^i = \tilde{S}_{n,out}^i - S_{n,out}^i = \xi_{S_{n,out}}^i. \quad \text{On the other hand}$$

$$x_{n+1,in}^i - M_{n+1,in}^i = \tilde{S}_{n+1,in}^i - S_{n+1,in}^i = \xi_{S_{n+1,in}}^i. \quad \text{Finally,}$$

$$M_{n+1,in}^i = M_{n,out}^i + M(CD). \quad \text{Therefore}$$

$$X_{n,out}^i = x_{n+1,in}^i - M(CD_n^i) + \xi_{S_{n,out}}^i - \xi_{S_{n+1,in}}^i \quad (13)$$

At slave $n+1$, the estimation of the RCF is quite similar to that in slave 1. Using (13) for the 2nd line:

$$\begin{aligned} RCF_{M/S_{n+1}}^i &= \frac{\hat{x}_{n,out}^i - \hat{x}_{n,out}^{i-1}}{\tilde{S}_{n+1,in}^i - \tilde{S}_{n+1,in}^{i-1}} = \frac{X_{n,out}^i - X_{n,out}^{i-1} - \gamma_{n,out}^i + \gamma_{n,out}^{i-1}}{\tilde{S}_{n+1,in}^i - \tilde{S}_{n+1,in}^{i-1}} \\ &= \bar{R}_{M/S_{n+1}}^{[x_{n+1,in}^i, \tilde{S}_{n+1,in}^i]} + \frac{\xi_{S_{n,out}}^i - \xi_{S_{n,out}}^{i-1} + \xi_{S_{n+1,in}}^i - \xi_{S_{n+1,in}}^{i-1} - \gamma_{n,out}^i + \gamma_{n,out}^{i-1}}{\tilde{S}_{n+1,in}^i - \tilde{S}_{n+1,in}^{i-1}} \quad (14) \\ &= \bar{R}_{M/S_{n+1}}^{[x_{n+1,in}^i, \tilde{S}_{n+1,in}^i]} + \frac{\eta_{n+1,in}^i}{\tilde{S}_{n+1,in}^i - \tilde{S}_{n+1,in}^{i-1}} \end{aligned}$$

Again, in the last line of (14), we use a Gaussian RV $\eta_{n+1,in}^i$ to approximate the sum of the random errors. With the result in (14), we can write **the state transition model** for slave $n+1$:

$$x_{n,in}^i = x_{n,in}^{i-1} + (\tilde{S}_{n,in}^i - \tilde{S}_{n,in}^{i-1}) \cdot RCF_{M/S_1}^i - \eta_1^i \quad (15)$$

The line delay connects the state variable $x_{n+1,in}^i$ with the estimate $X_{n,out}^i$:

$$X_{n,out}^i = x_{n+1,in}^i - \hat{S}_n(CD_n^j) \cdot \bar{R}_{M/S_n}^{CD_n^j} + \varepsilon_n^i \quad (16)$$

where ε_n^i is a Gaussian RV modeling all the uncertainties that arise since not $X_{n,out}^i$ is observed, but the estimate from the previous slave. We call (16) **coupling model**, not observation model like (11).

Using the state transition and coupling models described by (15) and (16), the estimation of the state variable $x_{n,in}^i$ is obtained by using a Kalman filter.

4. SIMULATION RESULTS

In order to verify our results, we have implemented the algorithm and simulated the synchronization protocol in a network with a line topology as shown in Fig. 1. Parameters for the simulation are summarized in Table I.

TABLE I
SIMULATION SETTINGS

Parameter	Value
Quartz precision	50ppm
Cable delay	100ns
Bridge delay	uniform 2ms+[5 125] μ s
Interval of Sync message	32ms
Interval of Delay request	8s
Stamping jitter	uniform [-40 40] ns
Jitter in line delay	uniform [-40 40] ns
Number of line delay averaging	8

The performance of the Kalman filter algorithm is evaluated through the synchronization error, i.e. the difference between the estimated master time and the true master time. Simulation results are shown in Fig. 4. For more remote slaves it takes time for the algorithm to converge. Fig. 5 shows the same results but using a different y-axis scale. It can be observed that the error oscillates around zero due to the uncertainties in the time stamping. The magnitude of the oscillation increases along the line since the latter slave element estimates the master time based on the estimates of the previous slaves so that error propagates.

5. CONCLUSIONS AND FUTURE WORK

This paper proposes a state-space model for a Kalman filter algorithm for time synchronization, using the time stamps provided by the PTP protocol. Performance of the algorithm

is evaluated through simulation results. Future work will be to compare this performance to that of other PTP based algorithms.

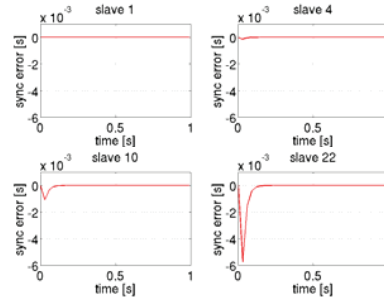


Fig. 4. Synchronization error

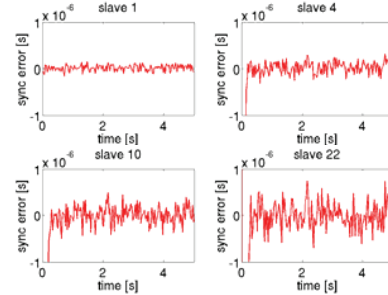


Fig. 5. Synchronization error

REFERENCES

- [1] D. L. Mills, "Internet time synchronization: The network time protocol", *Network Working Group Request for Comments*, 1989.
- [2] D. L. Mills, "Precision synchronization of computer network clocks", *ACM SIGCOMM Computer Communication Review*, Vol. 24, pp. 28-43, 1994.
- [3] IEEE.(2002). *IEEE Standard for a Precision Clock Synchronization Protocol for Networked Measurement and Control Systems*. IEEE, New York.
- [4] J. Jasperneite, K. Shehab, K. Weber. Enhancements to the time synchronization standard IEEE-1588 for a system of cascaded bridges. In: *Proc. of WFCS 2004*, pp. 239-44.
- [5] C. Na, D. Obradovic, R.L. Scheiterer, G. Steindl and F.J. Goetz, "Synchronization Performance of the Precision Time Protocol", *Proc. of ISPCS 2007*, Vienna, 2007.
- [6] R.L. Scheiterer, C. Na, D. Obradovic, G. Steindl and F. J. Goetz, "Synchronization performance of the Precision Time Protocol in industrial automation networks", accepted by the *ISPCS07 Special Issue of the IEEE Transactions on Instrumentation and Measurement*, 2008.